

Supporting Information

Electrostatically induced quantum point contacts in bilayer graphene

Hiske Overweg,^{*,†} Hannah Eggimann,[†] Xi Chen,[‡] Sergey Slizovskiy,^{‡,§} Marius Eich,[†] Riccardo Pisoni,[†] Yongjin Lee,[†] Peter Rickhaus,[†] Kenji Watanabe,[¶] Takashi Taniguchi,[¶] Vladimir Fal’ko,[‡] Thomas Ihn,[†] and Klaus Ensslin[†]

[†]*Solid State Physics Laboratory, ETH Zürich, CH-8093 Zürich, Switzerland*

[‡]*National Graphene Institute, University of Manchester, Manchester M13 9PL, UK*

[¶]*National Institute for Material Science, 1-1 Namiki, Tsukuba 305-0044, Japan*

[§]*On leave of absence from NRC “Kurchatov Institute” PNPI, Russia*

E-mail: overwegh@phys.ethz.ch

Fabrication and characterization

The geometry and mobility of both samples can be found in Table 1.

For the etching of the contacts, we use a recipe adapted from Ref. 1. We use a reactive ion etcher (Oxford Instruments RIE 80 Plus), with a mixture of CHF_3 gas (40 sccm) and O_2 (4 sccm). With an RF power of 60 W, the obtained etch rate of hBN is 45 nm/min. We carefully choose an etching time for each individual sample to make sure that the hBN is etched sufficiently for the contacts to reach the graphene layer, but not too far, since this would lead to a short between the contacts and the graphite back gate.

The deposition of Al_2O_3 was done in an atomic layer deposition system (Picosun Sunale R-150B) at a temperature of 150 °C with trimethylaluminum (TMA) and water as precursor gases.

For sample A we performed temperature dependent measurements of the resistance maximum for $(V_{\text{TG}}, V_{\text{BG}}) = -3.9, 4$ V, corresponding to a displacement field of 0.7 V/nm, and $(V_{\text{TG}}, V_{\text{BG}}) = -1.7, 2$ V, corresponding to a displacement field of 0.4 V/nm. The respective gap sizes were 55 meV and 16 meV. An indirect measure of the gap

Table 1: Characteristics of samples A and B

	sample A	sample B
graphite thickness (nm)	28	15
bottom BN thickness (nm)	38	53
top BN thickness (nm)	35	25
Al_2O_3 thickness (nm)	60	30
SG height (nm)	60	20
channel width (nm)	100	80
channel gate width (nm)	200	60
mobility (cm^2/Vs)	8×10^4	6×10^4

size is the resistance at charge neutrality. Figure S1a shows the resistance of sample A along several line cuts in Fig. 2a. The resistance at the charge neutrality point increases by orders of magnitude when a band gap is opened. The measurement was performed with a bias voltage of $V = 50 \mu\text{V}$. The data for the highest displacement field ($V_{\text{BG}} = 4$ V) has been omitted, because the high resistance peak cannot be reliably measured with a small bias voltage. Similar data for sample B is shown in Fig. S1b.

Simulation of the electrostatic potential

To get more insight in the electrostatic potential of the quantum point contact, we use a finite element simulator (COMSOL). The charge carrier sheet density $n(\vec{r})$ and the potential $V(\vec{r})$ are calculated self-consistently using Poisson's equation and the Thomas-Fermi approximation. The density of states is approximated by $D(E) = m^*/(\pi\hbar^2)\theta(E)$ with $m^* = 0.034m_e$ and θ the Heavyside step function, which limits the model to transport in the conduction band. We do not take the Mexican hat shape of the bilayer graphene band structure and the position dependent band gap into account. The quantization of states inside the one-dimensional channel, due to the lateral confinement, is also neglected.

Geometry

The geometry considered for the simulation is the same as for sample A (see main text and table 1). From AFM images of sample A it is apparent that the channel gate drops partially into the opening between the split gates. We therefore modelled the channel gate with an elliptical extension above the channel region (see Fig. S2). The width of this extension was 150 nm and the depth 30 nm, in agreement with the AFM images. When omitting the extension from the simulation, the channel gets depleted around $V_{CH} = -25$ V instead of the experimentally observed $V_{CH} = -12$ V. With the extension the channel gets depleted close to the experimentally observed value.

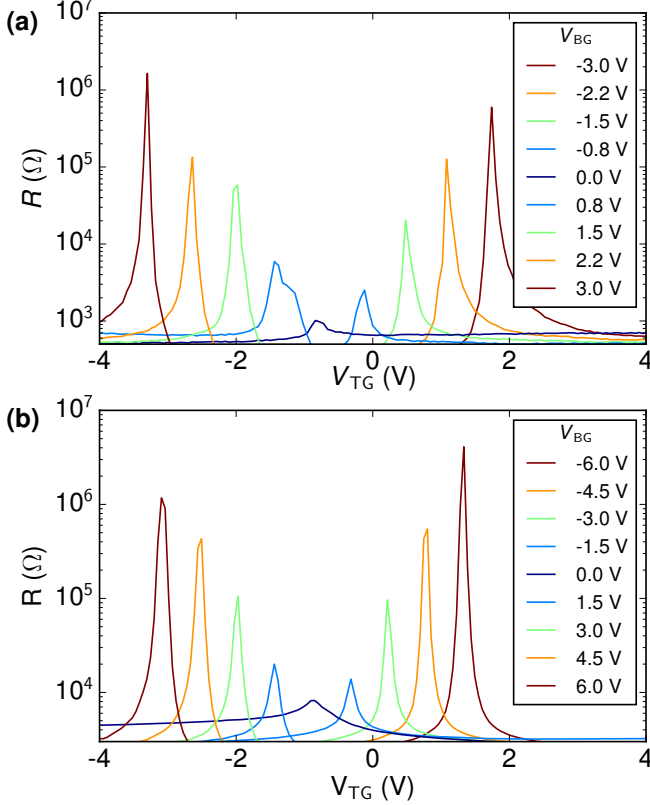


Figure S1: (a) Resistance of sample A as a function of top gate voltage for several back gate voltages. The resistance at the charge neutrality point increases by orders of magnitude when a band gap is opened. (b) Same for sample B

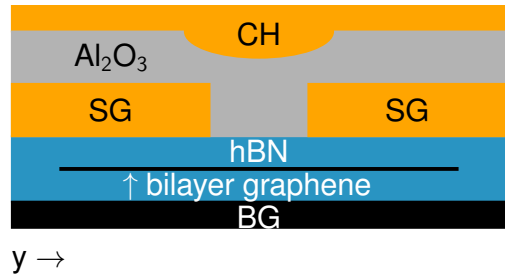


Figure S2: Cross section of the sample used for Comsol simulation. The channel gate has an elliptic extension above the channel.

Depletion below split gates

Figure S3 shows the calculated electrostatic potential along a line cut (black line in inset) under the split gate for $V_{BG} = 4$ V and various split gate voltages. At $V_{SG} = 0$ V, the potential is constant throughout the structure as expected. At $V_{SG} = -3.95$ V, the region under the split gates is depleted. This voltage is in agreement with the experimentally determined depletion voltage.

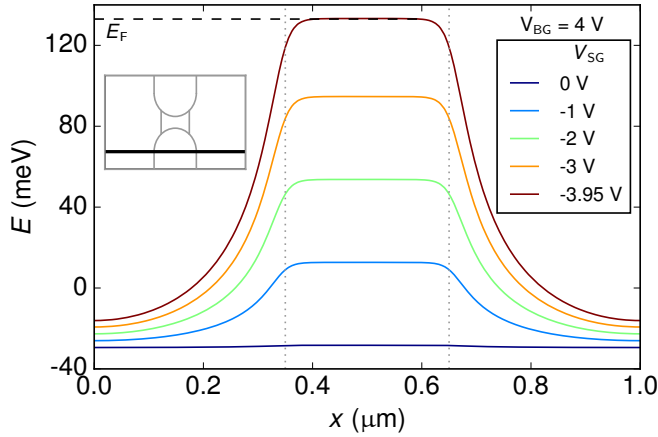


Figure S3: Calculated electrostatic potential along a line cut (black line in inset) under the split gate for $V_{BG} = 4$ V and various split gate voltages. The dotted lines indicate the extent of the split gates. At $V_{SG} = 0$ V, the potential is constant throughout the structure. At $V_{SG} = -3.95$ V, the region under the split gates is depleted.

Potential inside channel

In Fig. S4a the potential inside the channel is shown, for the case in which transport under the split gates is suppressed ($V_{BG} = 4$ V, $V_{SG} = -3.95$ V). For $V_{CH} = 0$ V, the potential can be approximated by a harmonic potential

$$V(y) = \frac{1}{2} m^* \omega_0^2 y^2$$

with an energy level separation of $\hbar\omega_0 = 8.4$ meV. For the gate voltage range of $V_{CH} = -10$ V - 12 V the energy level separation changes according to

$$\hbar\omega_0(V_{CH}) = 8.4 \text{ meV} + \alpha e V_{CH}$$

with $\alpha = 0.33 \times 10^{-3}$. The increased mode spacing with higher channel gate voltage can also be

observed in Fig. 3: the conductance rises less steeply for higher channel gate voltage.

Figure S4b shows the potential across the QPC. For the range of $V_{CH} = -12$ V - 8 V the positive curvature in y-direction and the negative curvature in x-direction lead to a conventional saddle point potential. Similar results were obtained for simulations of sample B.

Role of the bulk in magneto-transport

The density in the bulk of the sample is higher than the density inside the constriction for the entire range of Fig. 4. Only the edge modes that exist in both the bulk and the channel contribute to transport and the conductance is given by $G = \nu_{CH} e^2 / h$. We can see a modest influence of the bulk of the device whenever the bulk is at a transition between integer filling factors. Figure S5 shows the derivative of the conductance with respect to magnetic field as a function of V_{CH} and B for the same gate voltage settings as Fig. 4. The horizontal lines, which occur in a $1/B$ periodic fashion, correspond to Landau level transitions in the bulk of the sample. The filling factors of the bulk are indicated on the y-axis. Because of the high charge carrier density, no broken degeneracies are observed up to $B = 8$ T.

References

- (1) L Wang, I Meric, P Y Huang, Q Gao, Y Gao, H Tran, T Taniguchi, K Watanabe, L M Campos, D a Muller, J Guo, P Kim, J Hone, K L Shepard, and C R Dean, “One-dimensional electrical contact to a two-dimensional material.” *Science* **342**, 614–7 (2013).

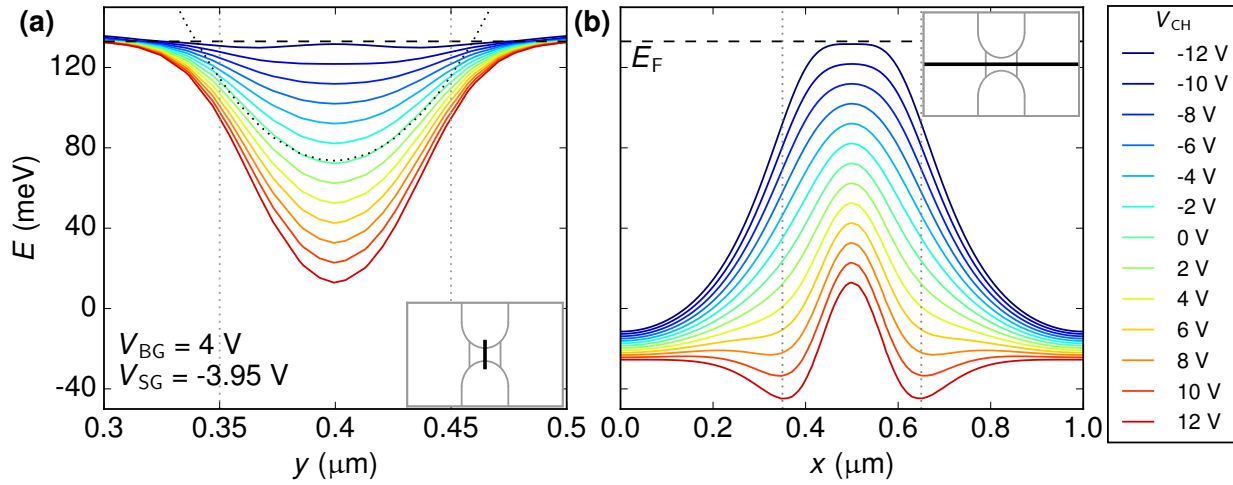


Figure S4: Potential landscape for $V_{BG} = 4$ V, $V_{SG} = -3.95$ V and various channel gate voltages. (a) Electrostatic potential across the channel, which can be approximated by a harmonic potential (dotted black line). The channel gets depleted close to the experimental depletion voltage of $V_{CH} = -12$ V. (b) Electrostatic potential along the channel. For the range of $V_{CH} = -12$ V - 8 V a conventional saddle point potential is observed.

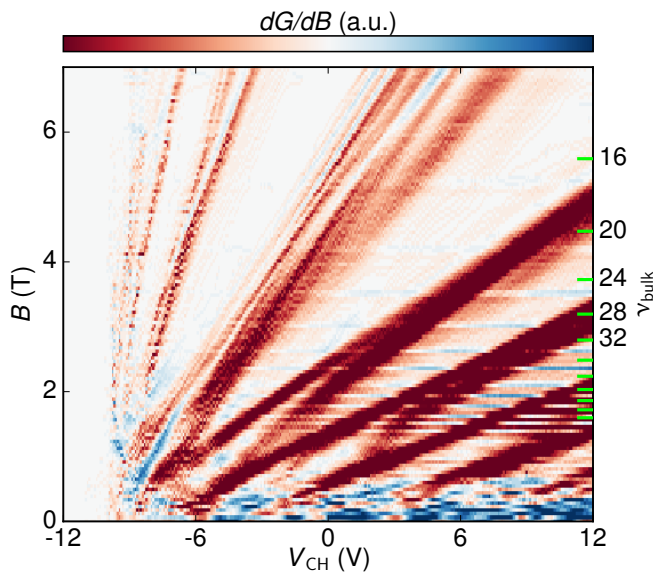


Figure S5: Derivative of the conductance with respect to magnetic field for the same gate voltage settings as Fig. 4c. $1/B$ periodic horizontal lines are observed, which correspond to Landau level transitions in the bulk of the sample.